

Equation of state of isospin-asymmetric nuclear matter in relativistic mean-field models with chiral limits

Wei-Zhou Jiang^{1,2}, Bao-An Li¹, and Lie-Wen Chen^{1,3}

¹ *Department of Physics, Texas A&M University-Commerce, Commerce, TX 75429, USA*

² *Institute of Applied Physics, Chinese Academy of Sciences, Shanghai 201800, China*

³ *Institute of Theoretical Physics, Shanghai Jiao Tong University, Shanghai 200240, China*

Abstract

Using in-medium hadron properties according to the Brown-Rho scaling due to the chiral symmetry restoration at high densities and considering naturalness of the coupling constants, we have newly constructed several relativistic mean-field Lagrangians with chiral limits. The model parameters are adjusted such that the symmetric part of the resulting equation of state at supra-normal densities is consistent with that required by the collective flow data from high energy heavy-ion reactions, while the resulting density dependence of the symmetry energy at sub-saturation densities agrees with that extracted from the recent isospin diffusion data from intermediate energy heavy-ion reactions. The resulting equations of state have the special feature of being soft at intermediate densities but stiff at high densities naturally. With these constrained equations of state, it is found that the radius of a $1.4M_{\odot}$ canonical neutron star is in the range of $11.9 \text{ km} \leq R \leq 13.1 \text{ km}$, and the maximum neutron star mass is around $2.0M_{\odot}$ close to the recent observations.

Keywords: Equation of state, nuclear matter, symmetry energy, relativistic mean-field models, chiral limits. PACS numbers: 21.65.+f, 26.60.+c, 11.30.Rd

1 Introduction

The Equation of State (EOS) of isospin asymmetric nuclear matter plays a crucial role in many important issues in astrophysics, see, e.g., Refs. [1, 2, 3]. It is also important for understanding both the structure of exotic nuclei and the reaction dynamics of heavy-ion collisions, see, e.g., Ref. [4]. Within the parabolic approximation, the energy per nucleon in isospin asymmetric nuclear matter can be written as $E/A = e(\rho) + E_{sym}(\rho)\delta^2$ where $e(\rho)$ is the EOS of symmetric nuclear matter, the $E_{sym}(\rho)$ is the symmetry energy and $\delta = (\rho_n - \rho_p)/\rho$ is the isospin asymmetry. Both the $e(\rho)$ and the $E_{sym}(\rho)$ are important in astrophysics although maybe for different issues.

For instance, the maximum mass of neutron stars is mainly determined by the EOS of symmetric nuclear matter $e(\rho)$ while the radii and cooling mechanisms of neutron stars are determined instead mainly by the symmetry energy E_{sym} [1, 5]. The nuclear physics community has been trying to constrain the EOS of symmetric nuclear matter using terrestrial nuclear experiments for more than three decades, see, e.g.[6], for a review. On the other hand, a similarly systematic and sophisticated study on the density dependence of the symmetry energy E_{sym} using heavy-ion reactions only started about ten years ago stimulated mostly by the progress and availability of radioactive beams[7]. Compared to our current knowledge about the EOS of symmetric nuclear matter, the symmetry energy E_{sym} is still poorly known especially at supra-normal densities [8] given the recent progress in constraining it at densities less than about $1.2\rho_0$ using the isospin diffusion data from heavy-ion reactions [9, 10, 11].

The aim of this work is to investigate the EOS of isospin asymmetric nuclear matter within the relativistic mean-field (RMF) model with in-medium hadron properties governed by the BR scaling. From the point of view of hadronic field theories, the symmetry energy is governed by the isovector meson exchange. Studying in-medium properties of isovector mesons is thus of critical importance for understanding the density dependence of the symmetry energy. We first construct model Lagrangians respecting the chiral symmetry restoration at high densities. The model parameters are adjusted such that the symmetric part of the resulting EOS at supra-normal densities is consistent with that required by the collective flow data from high energy heavy-ion reactions [6], while the resulting density dependence of the symmetry energy at sub-saturation densities agrees with that extracted from the recent isospin diffusion data from intermediate energy heavy-ion reactions [9, 10, 11]. The constrained EOS is then used to investigate several global properties of neutron stars.

2 Relativistic mean-field models with chiral limits

In-medium properties of the isovector meson ρ can be studied through the special symmetry breaking and restoration. The local isospin symmetry in the Yang-Mills field theory, where the ρ meson may be introduced as a gauge boson of the strong interaction, can serve as a possible candidate to study the in-medium properties of ρ meson. However, since πN interactions actually dominate the strong interaction in hadron phase, it was rather difficult to understand how the in-medium properties of the massive ρ meson could be consistent with the restoration of local

isospin symmetry. On the other hand, within the microscopic theory for the strong interaction, namely, the QCD which is a color SU(3) gauge theory, the chiral symmetry is approximately conserved. The spontaneous chiral symmetry breaking and its restoration can be manifested in effective QCD models. Based on the latter, Brown and Rho (BR) proposed the in-medium scaling law [12] implying that hadron masses and meson coupling constants in the Walecka model [13] approach zero at the chiral limit. The scaling was treated in the hadronic phase before the chiral symmetry restoration.

As an effective QCD field theory, the hidden local symmetry theory has been developed to include the ρ meson in addition to the pion in the framework of the chiral perturbative theory by Harada and Yamawaki [14, 15] and it is shown that the ρ meson becomes massless at the chiral limit. This supports the mass dropping scenario of the BR scaling. There are also experimental indication for the mass dropping, i.e., the dielectron mass spectra observed at the CERN SPS [16, 17], the ω meson mass shift measured at the KEK [18] and the ELSA-Bonn [19], as well as the analysis of the STAR data [20, 21]. However, data from the NA60 Collaboration for the dimuon spectrum [22] seem to favor the explanation of ρ meson broadening based on a many-body approach [23]. So far, the controversy is still unsettled [21]. The chiral symmetry and its spontaneous breaking are closely related to the mass acquisition and dropping of hadrons. Since the chiral symmetry is a characteristic of the strong interaction within the QCD, it is favorable to include in the RMF models effects of the chiral symmetry through the BR scaling law. However, this does not mean that the contribution of the many-body correlations [24] is excluded. Actually, the contribution of the many-body correlations can be included phenomenologically into the RMF models to reproduce the saturation properties of nuclear matter.

The in-medium ρ meson plays an important role in modifying the density dependence of the symmetry energy. For most RMF models that the ρ meson mass is not modified by the medium, the symmetry energy is almost linear in density. The introduction of the isoscalar-isovector coupling in RMF models can soften the symmetry energy at high densities [3]. Meanwhile, it reproduces the neutron-skin thickness in ^{208}Pb as that given by the non-relativistic models (about 0.22fm) [25], consistent with the available data [26]. In well-fitted RMF models that give a value of incompressibility $\kappa = 230$ MeV, a large coefficient of non-linear self-interacting ω meson term is required [25] and thus the naturalness breaks down. Moreover, the isoscalar-

isovector coupling in the RMF models increases the effective ρ meson mass with density, which leads the model to be far away from the chiral limit.

The Walecka model with the density-dependent parameters is the simplest version to incorporate the effects of chiral symmetry. The Lagrangian is written as

$$\begin{aligned} \mathcal{L} = & \bar{\psi}[i\gamma_\mu\partial^\mu - M^* + g_\sigma^*\sigma - g_\omega^*\gamma_\mu\omega^\mu - g_\rho^*\gamma_\mu\tau_3 b_0^\mu]\psi + \frac{1}{2}(\partial_\mu\sigma\partial^\mu\sigma - m_\sigma^{*2}\sigma^2) \\ & - \frac{1}{4}F_{\mu\nu}F^{\mu\nu} + \frac{1}{2}m_\omega^{*2}\omega_\mu\omega^\mu - \frac{1}{4}B_{\mu\nu}B^{\mu\nu} + \frac{1}{2}m_\rho^{*2}b_{0\mu}b_0^\mu \end{aligned} \quad (1)$$

where ψ, σ, ω , and b_0 are the fields of the nucleon, scalar, vector, and isovector-vector mesons, with their in-medium scaled masses $M^*, m_\sigma^*, m_\omega^*$, and m_ρ^* , respectively. The meson coupling constants and hadron masses with asterisks denote the density dependence, given by the BR scaling. The energy density and pressure read, respectively,

$$\mathcal{E} = \frac{1}{2}C_\omega^2\rho^2 + \frac{1}{2}C_\rho^2\rho^2\delta^2 + \frac{1}{2}\tilde{C}_\sigma^2(m_N^* - M^*)^2 + \sum_{i=p,n} \frac{2}{(2\pi)^3} \int_0^{k_{Fi}} d^3k E^*, \quad (2)$$

$$p = \frac{1}{2}C_\omega^2\rho^2 + \frac{1}{2}C_\rho^2\rho^2\delta^2 - \frac{1}{2}\tilde{C}_\sigma^2(m_N^* - M^*)^2 - \Sigma_0\rho + \frac{1}{3} \sum_{i=p,n} \frac{2}{(2\pi)^3} \int_0^{k_{Fi}} d^3k \frac{\mathbf{k}^2}{E^*} \quad (3)$$

where $C_\omega = g_\omega^*/m_\omega^*$, $C_\rho = g_\rho^*/m_\rho^*$, $\tilde{C}_\sigma = m_\sigma^*/g_\sigma^*$, $E^* = \sqrt{\mathbf{k}^2 + m_N^{*2}}$ with $m_N^* = M^* - g_\sigma^*\sigma$ the effective mass of nucleon, and k_F is the Fermi momentum. The incompressibility of symmetric matter can be expressed explicitly as [27]

$$\kappa = 9\rho \frac{\partial\mu}{\partial\rho} = 9\rho(C_\omega^2 + 2C_\omega\rho \frac{\partial C_\omega}{\partial\rho} + \frac{\partial E_F}{\partial\rho} - \frac{\partial\Sigma_0}{\partial\rho}) \quad (4)$$

where the chemical potential is given by $\mu = \partial\mathcal{E}/\partial\rho$ and the Fermi energy is $E_F = \sqrt{k_F^2 + m_N^{*2}}$. The rearrangement term is essential for the thermodynamic consistency to derive the pressure in (3) and its expectation value in the mean field Σ_0 is given by

$$\Sigma_0 = -\rho^2 C_\omega \frac{\partial C_\omega}{\partial\rho} - \rho^2 \delta^2 C_\rho \frac{\partial C_\rho}{\partial\rho} - \tilde{C}_\sigma \frac{\partial \tilde{C}_\sigma}{\partial\rho} (m_N^* - M^*)^2 - \rho_s \frac{\partial M^*}{\partial\rho}. \quad (5)$$

The density dependence of parameters is usually described by the scaling functions that are the ratios of the in-medium parameters to those in the free space. The choice of scaling functions and their coefficients are constrained by the saturation properties of nuclear matter and experimental data about the in-medium mass dropping of vector mesons. Moreover, we also use as a constraint the pressure within the density range $2-4.6\rho_0$ extracted from measurements of nuclear collective flows in heavy-ion collisions [6]. The scaling function may take the form [28]:

$$\Phi(\rho) = \frac{1}{1 + y\rho/\rho_0} \quad (6)$$

with $y = 0.28$ for the vector meson mass, giving $\Phi(\rho_0) = 0.78$ found in QCD sum rules [29]. Recently, in Ref. [30] where the memory effect in dimuon yield was studied by considering the mass dropping of ρ meson, the authors cited a scaling function [31]

$$\Phi(\rho) = 1 - y\rho/\rho_0 \quad (7)$$

with $y = 0.15$. Data extracted from the $\gamma - A$ reaction by the TAP collaboration indicate a value of $y \approx 0.13$ [32]. In addition, data from the KEK photon-induced nuclear reaction indicate that the ω meson mass dropping is about the same order of magnitude at the saturation density [33].

Song firstly built effective models based on the BR scaling using the scaling functions (6) for both hadron masses and vector coupling constants [28]. A reasonable incompressibility for nuclear matter was obtained by introducing the non-linear self-interacting meson terms with coefficients satisfying the hypothesis of *naturalness* that is originated from the chiral symmetry and QCD scaling [34, 35, 36, 37]. In Ref. [38], along the line of [28], the BR scaling function (6) was considered only for hadron masses with a small value of y in the RMF models to study nuclear matter properties. In a more recent work [39], the BR scaling function (6) was taken for the scalar and vector meson coupling constants with respective values of y , and the scaling function (7) was taken for hadron masses in the RMF models without the self-interacting meson interactions. Though the models built in these works can give rather good descriptions of nuclear saturation properties, the pressures calculated in the density region of $\rho = 2 - 4.6\rho_0$, however, are still far away from that extracted from measurements of nuclear collective flows in heavy-ion collisions [6]. People have already tried to improve the situation by including the non-linear meson self-interacting terms. Unfortunately, it is not satisfactory because even unreasonably large coefficients of non-linear meson terms that break down the hypothesis of *naturalness* can not reduce the pressure lower enough to pass the experimental pressure-density region.

The effective nucleon mass is not dominated by the BR scaling (at least at the normal nuclear matter density) since it is usually around $0.65M^*$ at normal density while the mass dropping given by the BR scaling is less than 15% ($y \leq 0.15$ in (7)). This implies that the scalar meson coupling constant that plays a crucial role in the effective nucleon mass can adopt a different density-dependent scaling from that of the vector meson. In particular, the high pressure predicted by various models at high densities should be lowered, and this requires the scalar coupling constant to decrease more slowly. Furthermore, if the scaling function (7) for the ω meson mass is preferred by experiments, one may take the same scaling function (7) for

Table 1: Parameter sets fitted at the saturation density $\rho_0 = 0.16\text{fm}^{-3}$. The vacuum hadron masses are $M = 938\text{MeV}$, $m_\sigma = 500\text{MeV}$, $m_\omega = 783\text{MeV}$ and $m_\rho = 770\text{MeV}$ except for $m_\sigma = 600\text{MeV}$ for the parameter set S3. The coupling constants given here are those at zero density. For parameter sets SL3 and S3, the non-linear σ self-interacting coefficients are introduced (see text). The parameter set SL1* has two more parameters $y_\rho = 0.654$ and $y_\omega = 0.0365$. The symmetry energy is fitted to 31.6MeV at $\rho = 0.16\text{fm}^{-3}$ for all models. The critical density ρ_c for the chiral symmetry restoration is given by the value y in (7) for zero hadron mass.

	g_σ	g_ω	g_ρ	y	x	$\kappa(\text{MeV})$	M^*/M	M_n^*/M	ρ_c/ρ_0
SL1	8.6388	10.4634	3.7875	0.126	0.234	230.0	1.0	0.679	7.94
SL1*	9.7414	12.5535	5.8644	0.126	0.238	230.0	1.0	0.600	7.94
SL2	6.1664	10.9682	3.9866	0.11	0.381	219.5	0.89	0.763	9.09
SL3	9.8627	12.4928	3.6128	0.126	-	250.0	1.0	0.620	7.94
S3[28]	5.3210	15.3134	3.6035	0.28	-	250.0	0.78	0.617	-

the coupling constant of ω meson to avoid the infinity of pressure at the chiral limit where the scalar density vanishes. In this way, the effect of density dependence from the vector meson part is cancelled out since the energy density (3) only relies on the ratios C_ω and C_ρ . Generally, we may take the scaling functions for the coupling constants of vector mesons as

$$\Phi_\rho(\rho) = \frac{1 - y\rho/\rho_0}{1 + y_\rho\rho/\rho_0}, \quad \Phi_\omega(\rho) = \frac{1 - y\rho/\rho_0}{1 + y_\omega\rho/\rho_0}. \quad (8)$$

For hadron masses (including nucleons, if they have), (7) is taken with the same value of y used in (8). For the σ meson coupling constant, the same form as (6) is taken but with a coefficient denoted by x :

$$\Phi_\sigma(\rho) = \frac{1}{1 + x\rho/\rho_0}. \quad (9)$$

3 Results and discussions

We first adjust the parameters to reproduce the saturation properties including the binding energy per nucleon $E/A - M = -16$ MeV, the zero pressure, the incompressibility κ and the effective nucleon mass m_N^* at saturation density $\rho_0 = 0.16\text{fm}^{-3}$. The resulting parameter sets SL1 and SL2 and the corresponding saturation properties are tabulated in Table 1. In SL1 the nucleon mass scaling is not considered and the effective nucleon mass is just $m_N^* = M - g_\sigma^*\sigma$. In SL2, the nucleon mass scaling is included, and a much larger effective nucleon mass at normal density is obtained. There are just two coefficients x and y used in the scaling functions in SL1 and SL2. Without the inclusion of the non-linear meson self-interacting terms, the saturation

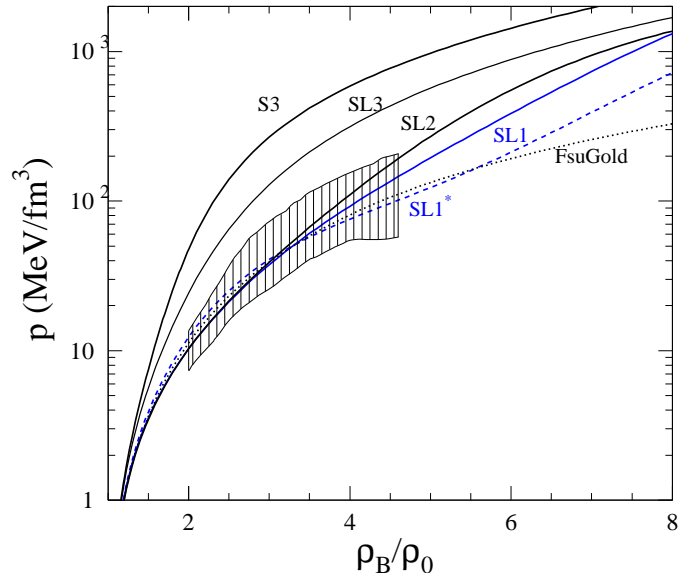


Figure 1: The pressure as a function of density for different models. The shaded region is given by experimental error bars[6].

properties at $\rho_0 = 0.16\text{fm}^{-3}$ (see Table 1) and the pressure within the density region $\rho = 2-4.6\rho_0$ are both nicely reproduced with the SL1 and SL2 (see Fig. 1). It is worth mentioning that the vector potential which is quadratic in density for the constant C_ω is known to result in a higher pressure above the experimental region. The softening of the pressure here is attributed to the contribution of rearrangement terms. For the SL1, only the rearrangement term from the σ meson survives.

The parameter set SL3 does not consider the scaling of scalar meson coupling constant but includes in the Lagrangian the non-linear σ self-interacting terms $U(\sigma) = g_2\sigma^3/3 + g_3\sigma^4/4$ with coefficients $g_2 = 23.095$ and $g_3 = -29.678$. Though these large coefficients are needed to fit the saturation properties, they seem to be inconsistent with the hypothesis of *naturalness* [35, 36]. In S3, we introduce a $g_2 = -1.096$ to obtain the given κ in Table 1. This is a little different

from the original one [28]. As a comparison, we can see in Fig.1 that the SL3 and S3 parameter sets are not consistent with the pressure constrained by the collective flow data.

With (3), the symmetry energy in the RMF models can be derived as

$$E_{sym} = \frac{1}{2} \frac{\partial^2(\mathcal{E}/\rho)}{\partial\delta^2} = \frac{1}{2} C_\rho^2 \rho + \frac{k_F^2}{6E_F}. \quad (10)$$

It consists of contribution from the ρ meson (potential part) and nucleons (kinetic part). In SL1 and SL2, we adopt the same scaling function for coupling constants of ρ and ω mesons: $\Phi_\rho(\rho) = \Phi_\omega(\rho) = 1 - y\rho/\rho_0$. In this way, the ratio C_ρ is just a constant that does not rely on the density. An almost linear dependence of the symmetry energy on the density is expected from Eq.(10). The symmetry energy as a function of density is shown in Fig.2. In Refs. [10, 11], the symmetry energy extracted from the isospin diffusion data is parameterized as $E_{sym} = 31.6(\rho/\rho_0)^\gamma$ with $0.69 \leq \gamma \leq 1.05$. All the parameter sets based on the BR scaling discussed above lead to the symmetry energies between those parameterized with $\gamma = 0.69$ and 1.05 in the whole density region. In Ref. [11], the authors pointed out that with the in-medium nucleon-nucleon cross sections, a symmetry energy of $E_{sym}(\rho) = 31.6(\rho/\rho_0)^{0.69}$ for $\rho < 1.2\rho_0$ was found most acceptable compared to the isospin diffusion data. However, the symmetry energy at higher densities is not constrained at all. It is thus interesting to examine predictions within the RMF models with the chiral limit at high densities.

Our strategy is to first fit the symmetry energies constrained at low densities by modifying the coefficient y_ρ in (8), and then predict the symmetry energy at high densities. The modified symmetry energy is shown in Fig.2 with the dashed blue curve denoted as SL1*. Considering the nucleon effective mass at normal density is a little large in SL1, we introduce a coefficient y_ω in (8) to reduce it to the value of $0.6M$. The new parameter set is called SL1* and also listed in Table 1. The different parameterizations in SL1 and SL1* lead to significantly difference in pressure at high densities as shown in Fig.1. However, the suppression of the symmetry energy in SL1* at high densities is dominated by the density dependence of the ratio C_ρ in (10). This can be seen by comparing results shown in Table 1 and Fig.2 that the density dependence of the symmetry energy does not change much by the different nucleon effective masses of various parameter sets. In the density-dependent RMF model [24], the dropping of ratios like the C_ω or C_ρ is induced by the many-body correlation contributions. Though the mechanism is different from the present study, the correlation effect beyond the mean-field approximation may play some role in obtaining the coefficients y_ρ and y_ω .

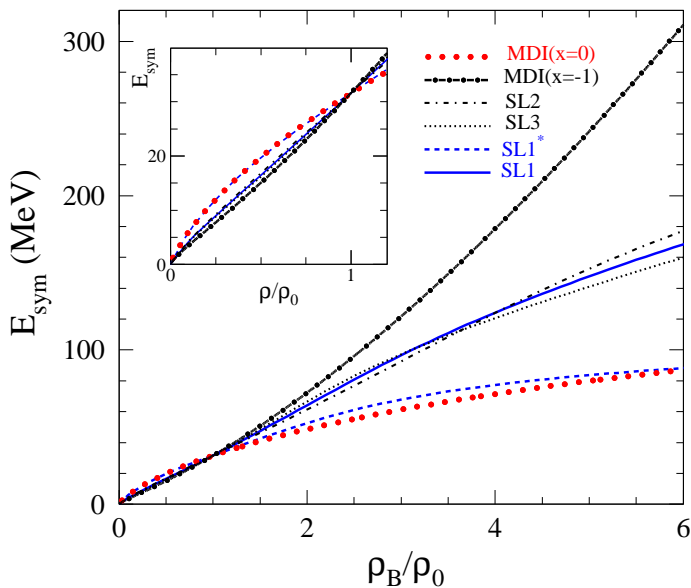


Figure 2: The symmetry energy as a function of density for different models. The MDI($x=0$) and MDI($x=-1$) results are taken from [10].

The symmetry energy at high densities from the MDI interaction with $x=0$ is quite close to that given by the SL1*. This is not surprising since the SL1* is rendered to have the same symmetry energies as the MDI($x=0$) at low densities. On the other hand, this justifies the consistency of the symmetry energy given by both models at high densities. One can freely adjust y_ρ to fit the symmetry energies given by the MDI($x=-1$) model at low densities and then examine the behavior at high densities. However, the C_ρ will increase with density by doing so, which is contrary to the empirical cases [24, 25]. Therefore, based on the BR scaling the symmetry energy at high densities is expected to be between those given by the SL1 and the SL1*.

We now turn to the astrophysical implications of the EOS's constrained above. Generally speaking, these EOS's have the special features of being soft at moderate densities and stiff at

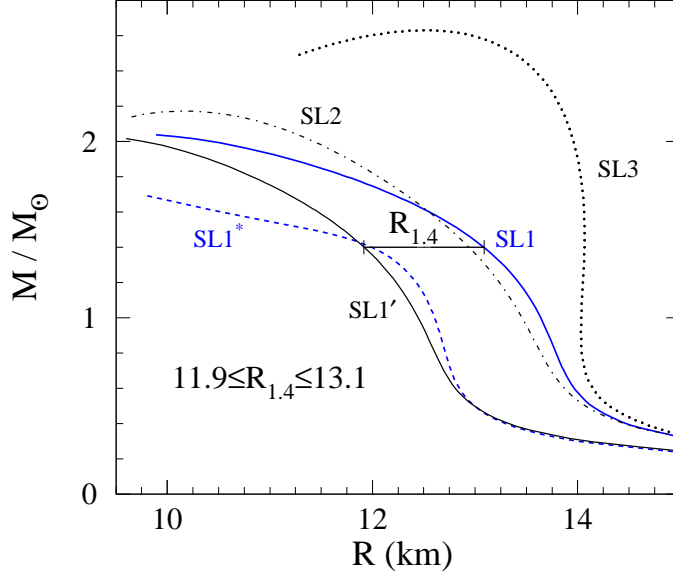


Figure 3: The neutron star mass versus the radius for various models. The parameter set SL1' is just the same as the SL1 but with $y_\rho = 0.526$.

high densities (see Fig. 1). It is thus interesting to compare predictions using these EOS's with the recent astrophysical observations. Recent studies on the millisecond pulsar PSR J0751+1807 suggest that it has a mass of $2.1 \pm 0.2^{(+0.4)}_{(-0.5)}$ with 1σ (2σ) confidence[40]. Since the maximum mass of neutron star is more sensitive to the EOS at high densities, this requires a rather stiff EOS at least at high densities. In Fig.3, we plot the mass-radius correlation of neutron stars obtained from solving the standard TOV equation. In the models with chiral limits, hadron masses approach zero at certain critical baryon densities (see Table 1). The maximum central energy density in a neutron star is that calculated at the maximum baryon density. With SL1, the maximum neutron star mass is $2.04M_\odot$ with a radius of $R=9.89\text{km}$. With SL2, these two observables are $2.17M_\odot$ and $R=10.13\text{km}$, respectively. As the nucleon effective mass at normal density is reduced by introducing the parameter y_ω , the maximum neutron star mass

also drops. This is owing to that the introduction of y_ω softens the EOS at high densities and the energy density at the critical density is thus lowered. With SL1*, the nucleon effective mass is $M_n^* = 0.6M$ at ρ_0 , and the maximum neutron star mass is $1.7M_\odot$. For a moderate value of $M_n^* = 0.65M$, we can obtain a moderately larger neutron star mass $1.94M_\odot$. Recent measurements on the neutron star EXO 07482-676 gave a mass of $M = 2.10 \pm 0.28M_\odot$ and a radius of $13.8 \pm 1.8\text{km}$ [41]. The author indicated that the existence of such a massive neutron star rules out all the soft EOS's of neutron-star matter. Among the models studied here, only the parameter set SL3 can give values close to the measurement for the EXO 07482-676. However, the parameter set SL3 gives a pressure at $\rho \leq 4.6\rho_0$ that is too strong compared to that constrained by the collective flow data in heavy-ion collisions [6]. For the other parameter sets, the radii of maximum mass neutron stars are just around 10km, which is below that given in [41], though the maximum mass can be within the error bars of the measurement (except for SL1*).

Compared to the EOS obtained using the FSUGold parameter set [25] the EOS's in the present study are stiffer at high densities although they have the same incompressibility $\kappa = 230$ MeV at normal density (see Fig.1). The EOS's obtained here thus also result in larger maximum masses of neutron stars. In Ref. [5], the authors predicted a radius span of $11.5\text{km} < R < 13.6\text{km}$ for the $1.4M_\odot$ canonical neutron star. Using the EOS's obtained in the present work, we obtain here a radius span of $11.9\text{km} < R < 13.1\text{km}$ for the $1.4M_\odot$ neutron star, which is comparable with that obtained in Ref. [5].

4 Summary

In summary, within the RMF framework we have constructed several new model Lagrangians using in-medium hadron properties according to the Brown-Rho scaling due to the chiral symmetry restoration at high densities. The model parameters are determined such that the symmetric part of the resulting EOS's at supra-normal densities are consistent with that required by the collective flow data from high energy heavy-ion reactions, while the resulting density dependence of the symmetry energy at sub-saturation densities agrees with that extracted from the recent isospin diffusion data from intermediate energy heavy-ion reactions. The rearrangement terms are found to play an important role in softening the EOS at moderate densities. The symmetry energy depends on the in-medium hadron properties that are characteristic of the

chiral symmetry restoration at the critical density according to the BR scaling. The resulting EOS's are then used to examine global properties of neutron stars. It is found that the radius of a $1.4M_{\odot}$ neutron star is in the range of $11.9\text{km} \leq R \leq 13.1\text{km}$. Compared to other EOS's, the current EOS's have the special feature of being soft at intermediate densities but stiff at high densities naturally. This feature is important to produce a heavier maximum neutron star mass around $2.0M_{\odot}$ consistent with recent observations.

Acknowledgement

We thank P. Krastev and G.C. Yong for useful discussions. The work was supported in part by the US National Science Foundation under Grant No. PHY-0652548, the Research Corporation, the National Natural Science Foundation of China under Grant Nos. 10405031, 10575071 and 10675082, MOE of China under project NCET-05-0392, Shanghai Rising-Star Program under Grant No. 06QA14024, the SRF for ROCS, SEM of China, and the Knowledge Innovation Project of the Chinese Academy of Sciences under Grant No. KJXC3-SYW-N2.

References

- [1] J. M. Lattimer and M. Prakash, Phys. Rep. **333**, 121 (2000); Astrophys. J. **550**, 426 (2001); Science **304**, 536 (2004).
- [2] A. W. Steiner, M. Prakash, J. M. Lattimer and P. J. Ellis, Phys. Rep. **411**, 325 (2005).
- [3] C.J. Horowitz, J. Piekarewicz, Phys. Rev. Lett. **86**, 5647 (2001).
- [4] Isospin Physics in Heavy-Ion Collisions at Intermediate Energies, Eds. Bao-An Li and W. Udo Schröder (Nova Science Publishers, Inc, New York, 2001).
- [5] B. A. Li and A. W. Steiner, Phys. Lett. B **642**, 436 (2006).
- [6] P. Danielewicz, R. Lacey, W. G. Lynch, Science **298**, 1592, (2002).
- [7] B.A. Li, C.M. Ko and Z.Z. Ren, Phys. Rev. Lett. **78**, 1644 (1997).
- [8] B. A. Li, Phys. Rev. Lett. **85**, 4221 (2000); *ibid.* **88**, 192701 (2002).
- [9] M. B. Tsang et.al. Phys. Rev. Lett. **92**, 062701 (2004).

- [10] L. W. Chen, C. M. Ko, B. A. Li, Phys. Rev. Lett. **94**, 032701 (2005).
- [11] B. A. Li, L. W. Chen, Phys. Rev. **C72**, 064611 (2005).
- [12] G. E. Brown, M. Rho, Phys. Rev. Lett. **66**, 2720 (1991).
- [13] B. D. Serot, J. D. Walecka, Adv. Nucl. Phys. **16**, 1 (1986).
- [14] M. Harada and K. Yamawaki, Phys. Rept. **381**, 1 (2003).
- [15] M. Harada, hep-ph/0703238.
- [16] G. Agakishiev et al., Phys. Rev. Lett. **75**, 1272 (1995).
- [17] G. Q. Li, C. M. Ko and G. E. Brown, Phys. Rev. Lett. **75**, 4007 (1995).
- [18] M. Naruki et al., Phys. Rev. Lett. **96**, 092301 (2006).
- [19] D. Trnka et al., Phys. Rev. Lett. **94**, 192303 (2005).
- [20] E. V. Shuryak and G. E. Brown, Nucl. Phys. A **717**, 322 (2003).
- [21] G. E. Brown, J. W. Holt, C.-H. Lee, M. Rho, Phys. Rep. **439**, 161 (2007).
- [22] S. Damjanovic et al. (NA60 Collaboration), Phys. Rev. Lett. **96**, 162302 (2006).
- [23] H. V. Hees, R. Rapp, Phys. Rev. Lett., **97**, 102301 (2006).
- [24] F. Hofmann, C. M. Keil, H. Lenske, Phys. Rev. **C64**, 034314 (2001).
- [25] B. G. Todd-Rutel, J. Piekarewicz, Phys. Rev. Lett. **95**, 122501 (2005).
- [26] B. Klos, et.al., nucl-ex/0702016.
- [27] Y. Iwasaki, H. Kouno, A. Hasegawa, M. Nakano Int. J. Mod. Phys. **E9**, 459 (2000).
- [28] C. Song, Phys. Rep. **347**, 289 (2001).
- [29] X. M. Jin, D. B. Leinweber, Phys. Rev. **C 52**, 3344 (1995).
- [30] B. Schenke, C. Greiner, Phys. Rev. Lett. **98**, 022301 (2007).
- [31] G. E. Brown and M. Rho, nucl-th/0509001; *ibid.* nucl-th/0509002.

- [32] D. Trnka et al., Phys. Rev. Lett. **94**, 192303 (2005).
- [33] M. Naruki et al., Phys. Rev. Lett. **96**, 092301 (2006).
- [34] A. Manohar, H. Georgi, Nucl. Phys. B **234**, 189 (1984).
- [35] D. G. Madland, T. J. Burvenich, J. A. Maruhn, P.-G. Reinhard, Nucl. Phys. A **741**, 52 (2004).
- [36] H. Uechi, Nucl. Phys. A **780**, 247 (2006).
- [37] S. Weinberg, Phys. Lett. B **251**, 288 (1990).
- [38] B. Liu, H. Guo, V. Greco, et. al. Eur. Phys. J. A **22**, 337 (2004).
- [39] S. S. Avancini, D. P. Menezes, Phys. Rev. C **74**, 015201 (2006).
- [40] D. J. Nice, E. M. Splaver, I. H. Stairs, et.al., Astrophys. J. **634**, 1242 (2005).
- [41] F. Özel, Nature **441**, 1115 (2006).